Electronic Supplementary Information

AIE-based Donor-Acceptor-Donor Fluorenone Compound as multi-functional luminescence materials

Xianchao Du[a,b,d‡], Huifang Su[c‡], Li Zhao[b‡], Xiaojing Xing[a], Bingnan Wang[d], Dongfang Qiu[*a], Jinyi Wang[*b] and Mao-Sen Yuan[*b]

[a] College of Chemistry and Pharmaceutical Engineering, Nanyang Normal University, Nanyang, Henan 473061, P. R. China

[b] College of Chemistry & Pharmacy, Northwest A&F University, Yangling, Shanxi 712100, P. R. China

[c] Department of Orthopaedic Surgery, The First Affiliated Hospital of Zhengzhou University, Zhengzhou, Henan 450052, P. R. China.

[d] State Key Laboratory of Luminescent Materials and Devices, Guangdong Provincial Key Laboratory of Luminescence from Molecular Aggregates, Center for Aggregation-Induced Emission, South China University of Technology, Guangzhou, Guangdong 510640, P. R. China.

Synthesis of MBPF

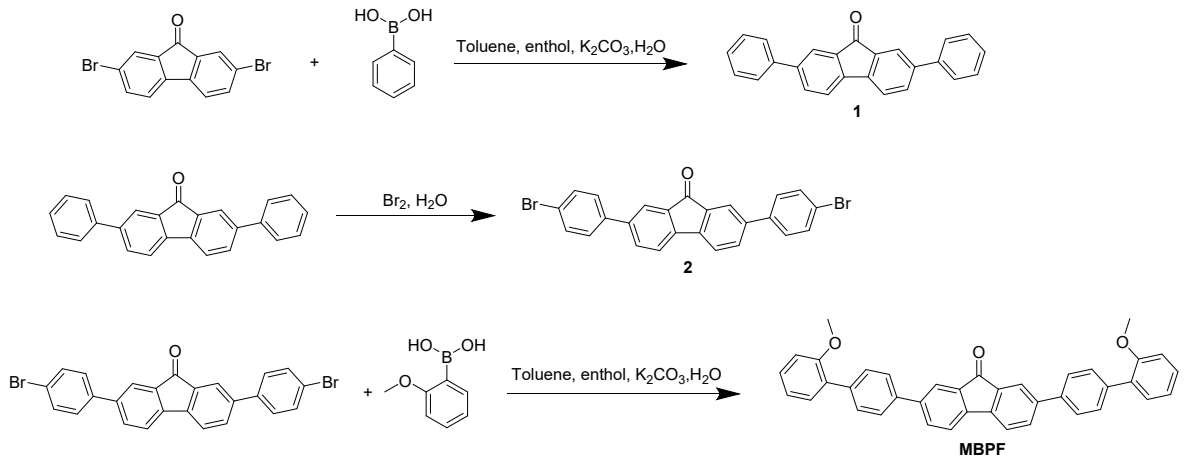

Scheme S1. Synthetic routes to **MBPF**.

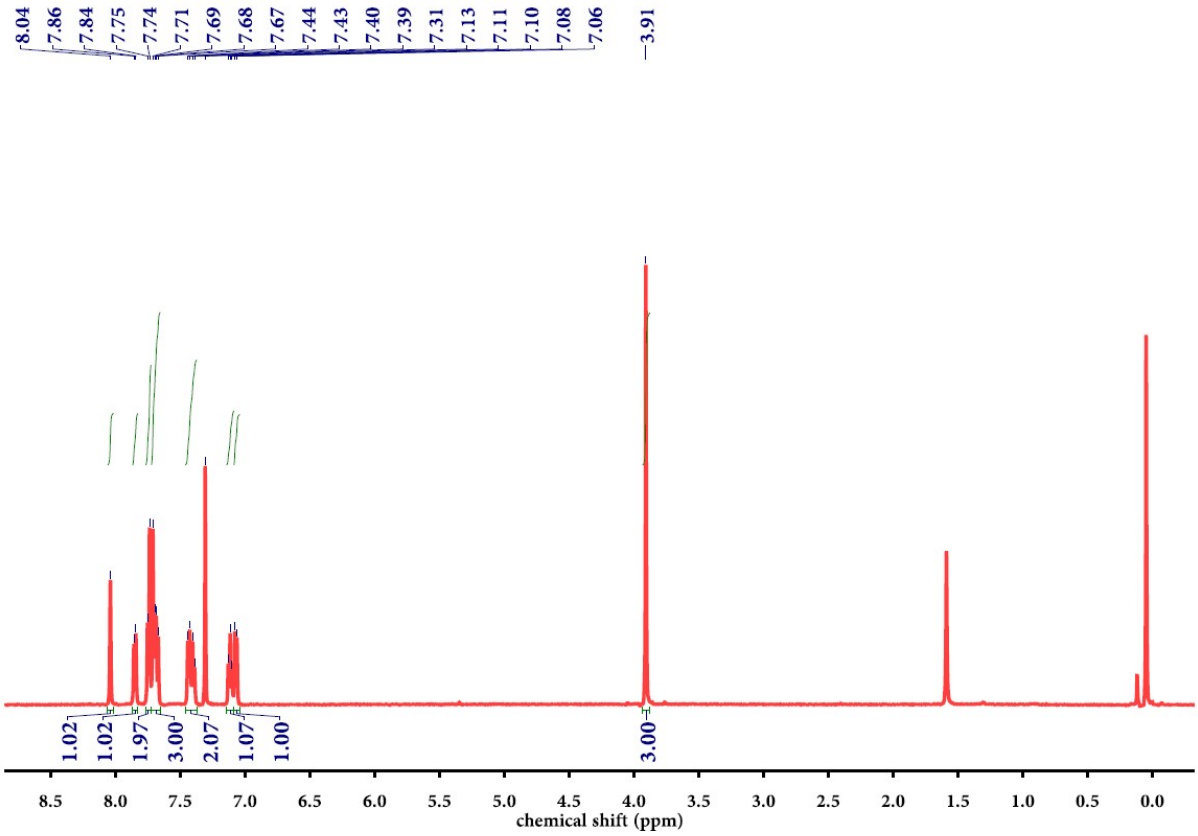

Fig. S1 ^{1}H NMR spectrum (500 MHz, $CDCl_3$) of compound **MBPF**.

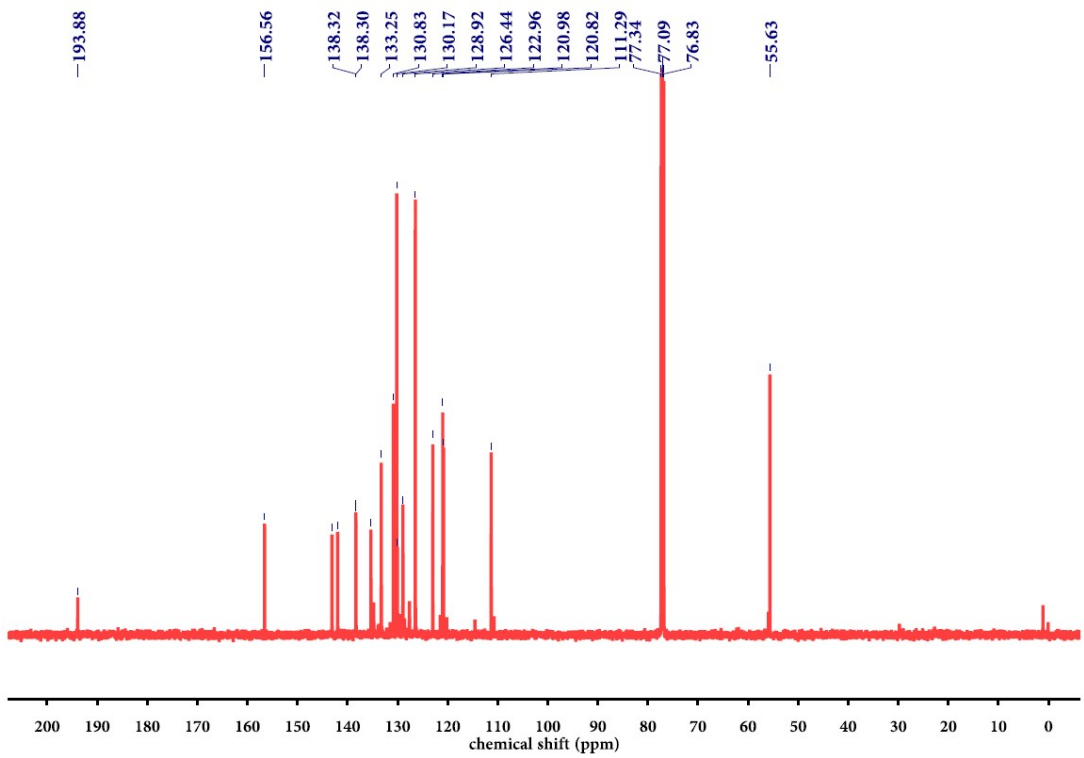

Fig. S2 ^{13}C NMR spectrum (126 MHz, $CDCl_3$) of compound **MBPF**.

Fig. S3 HRMS spectrum of **MBPF**.

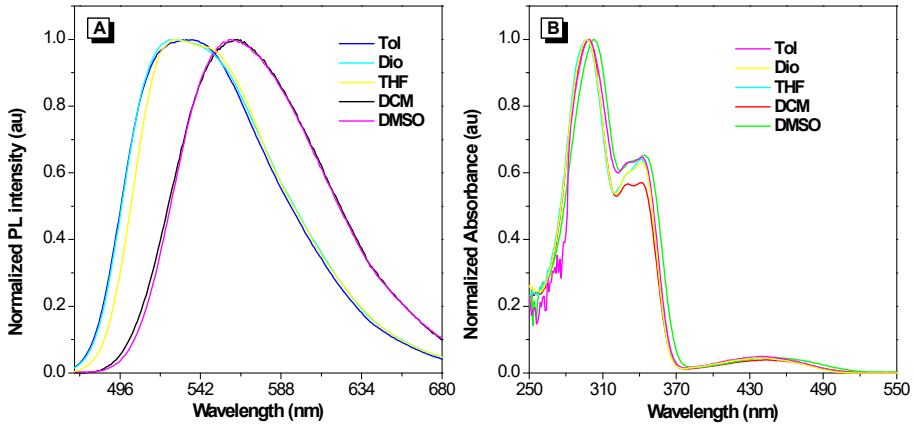

Fig. S4 Normalized PL spectra (A) and absorbance spectra (B) of **MBPF** in different solvents. Tol, toluene; Dio, dioxane; THF, tetrahydrofuran; DCM, dichloromethane; DMSO, dimethylsulfoxide.

Table S1. Photophysical properties of **MBPF** in various solvents

Solvent[a]	λ_{abs}[b]	λ_{em}[c]	**Φ(%)**[d]	**τ**[e]
Tol	297	530	0.25	6.19
Dio	297	527	0.15	9.26
THF	298	529	0.16	9.86
DCM	299	559	0.07	2.91
DMSO	303	563	0.07	3.01

[a] Abbreviations: Tol, Toluene; Dio, Dioxane; THF, Tetrahydrofuran; DCM, Dichloromethane; DMSO, Dimethyl sulfoxide; [b] λ_{abs}, absorption maximum, [c] λ_{ex}, emission maximum, [d] Fluorescence quantum yield, [e] Fluorescence lifetime.

Table S2. Spectroscopic data for compound **MBPF**

	Solution in THF[a]				Crystalline powder		
	λ_{abs}(nm)	λ_{em}(nm)	Φ^c	τ^d(ns)	λ_{em}(nm)	Φ	τ(ns)
Y-MBPF[b]					532	0.43	11.41
O-MBPF	298, 340	530	0.16	9.86	558	0.35	9.05
R-MBPF					590	0.36	9.55

[a] With c = 1.0 x 10^{-5} mol L^{-1}. [b] The amorphous, red crystal and orange crystal of compound **MBPF** are named **Y-MBPF**, **O-MBPF** and **R-MBPF**, respectively. [c] Fluorescence quantum yield. [d] Fluorescence lifetime.

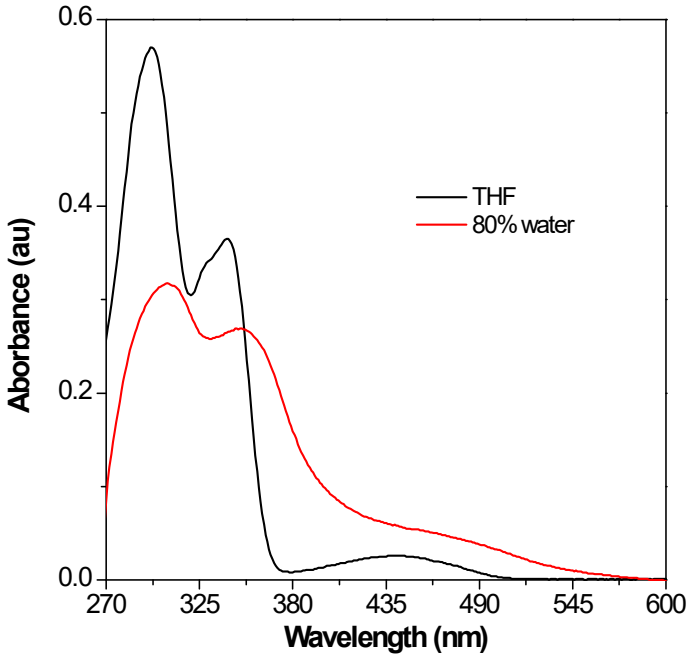

Fig. S5 The absorbance spectra of **MBPF** in pure THF and 80% water/THF.

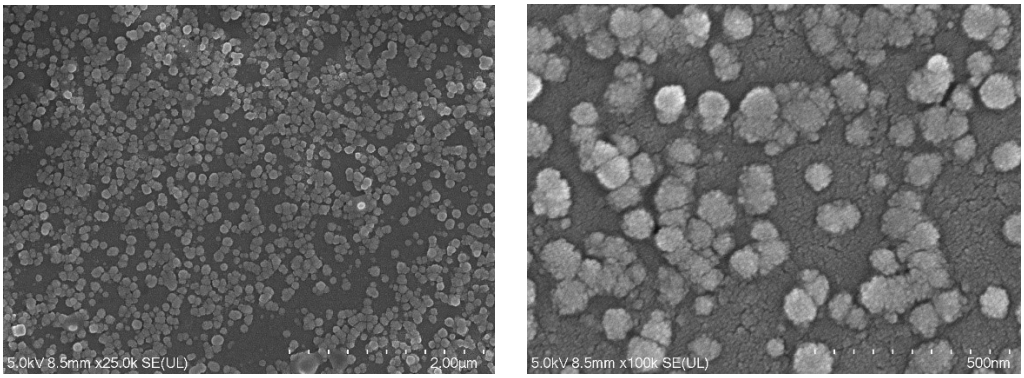

Fig. S6 The SEM of **MBPF** in water/THF (90 vol% water).

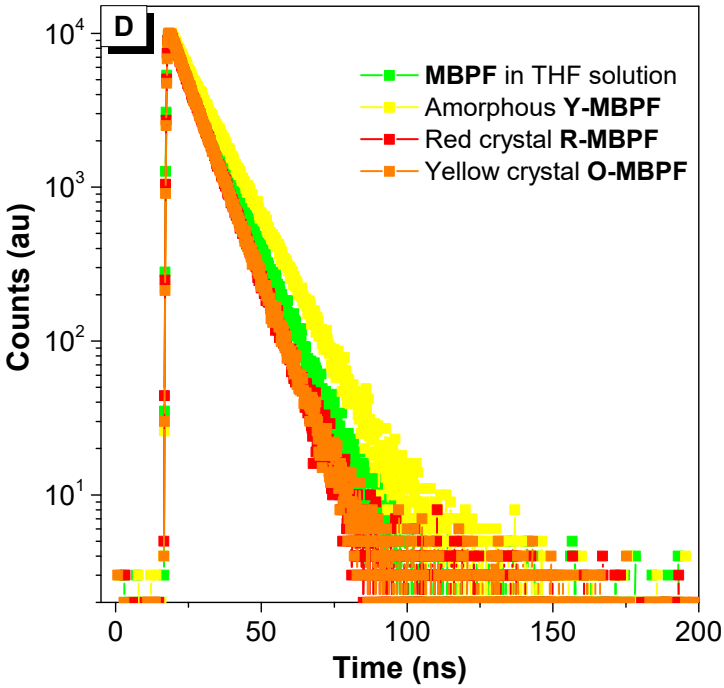

Fig. S7 The fluorescence decay profiles of **MBPF** in THF, Orange crystal **O-MBPF**, Red crystal **R-MBPF** and amorphous **Y-MBPF**.

Table S3. Selected crystallographic data for O-MBPF and R-MBPF.

crystals	**O-MBPF**	**R-MBPF**
formula	$C_{39}H_{28}O_3$	$C_{39}H_{28}O_3$
fw[g·mol^{-1}]	544.61	544.61
crystal color	Orange	Red
crystal system	Monoclinic	Triclinic
space group	$P2_1/c$	$P\text{-}1$
a [Å]	10.028(11)	10.0977(9)
b[Å]	17.169(19)	13.5881(12)
c [Å]	32.96(4)	22.1586(19)
β[º]	94.169(19)	78.4920(10)
V [Å^3]	5660(11)	2853.9(4)
Z	8	4
ρ_{calcd} [g/cm^3]	1.278	1.268
μ[mm^{-1}]	0.080	0.079
T[K]	298(2)	298(2)
θ_{min}-θ_{max} [º]	2.20-25.02	2.29 –25.02
$R/wR[I > 2\sigma_{(1)}]$	0.1058/0.1393	0.0507/0.0607

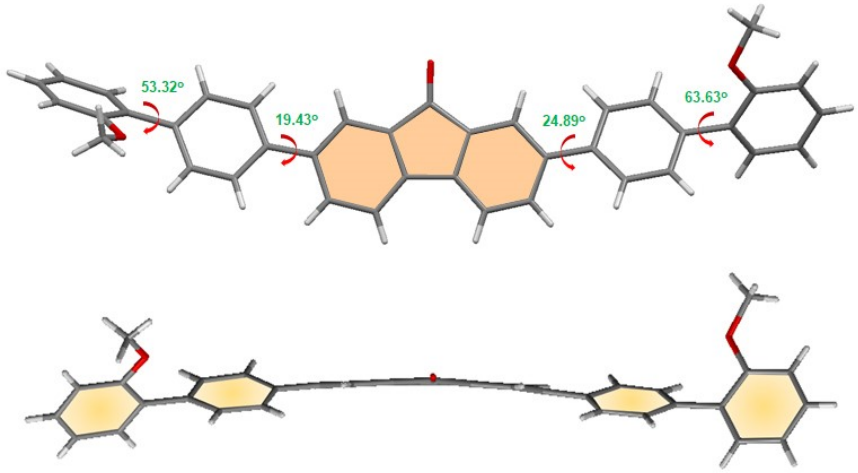

Fig. S8 The single crystal structure of **O-MBPF**.

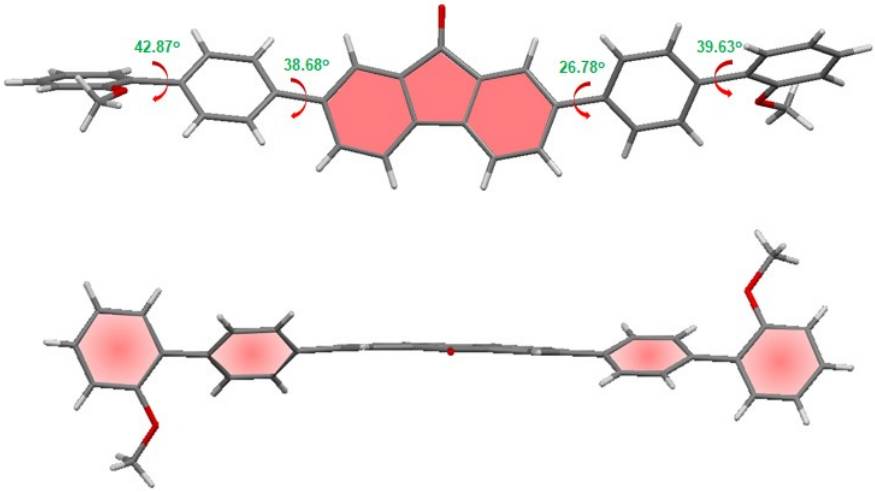

Fig. S9 The single crystal structure of **R-MBPF**.

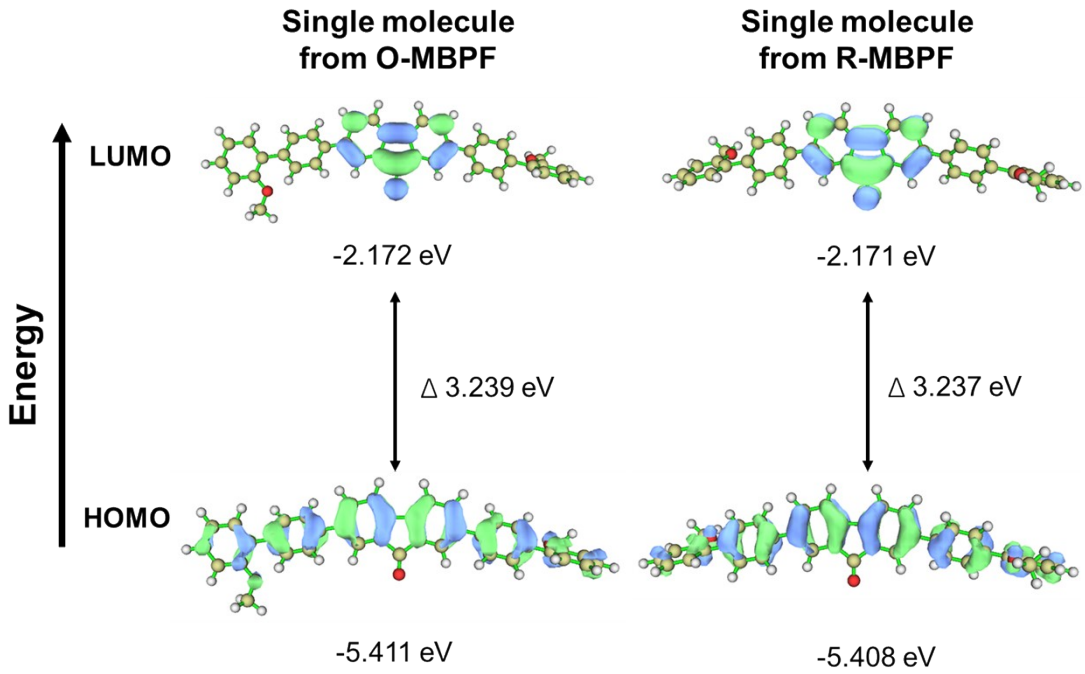

Fig. S10 Calculated HOMO and LUMO electron cloud for orange crystal **O-MBPF** and red crystal **O-MBPF** with their relative energy according to TD-DFT calculation.

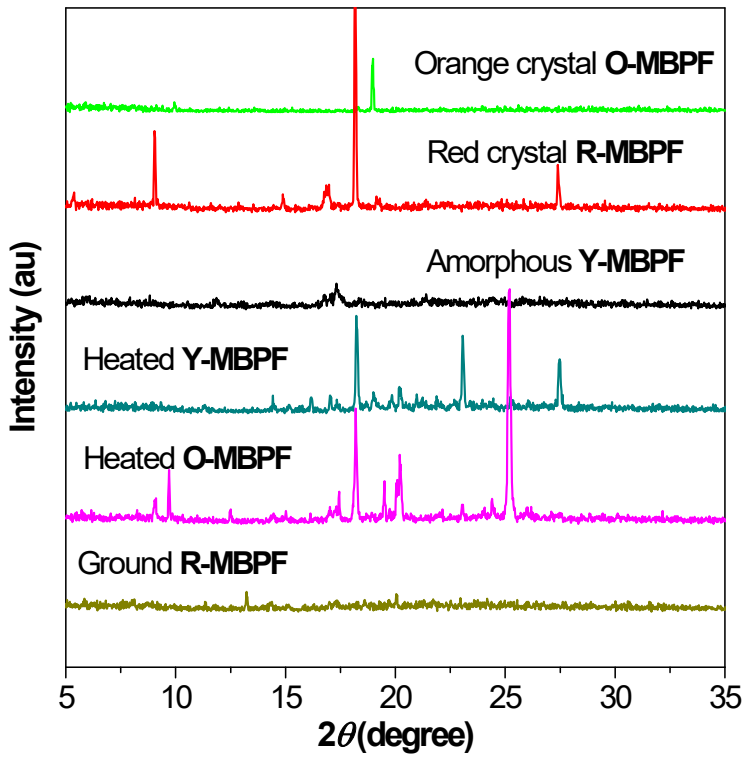

Fig. S11 Powder XRD profiles of the Orange crystal **O-MBPF**, Red crystal **R-MBPF** and amorphous **Y-MBPF**.

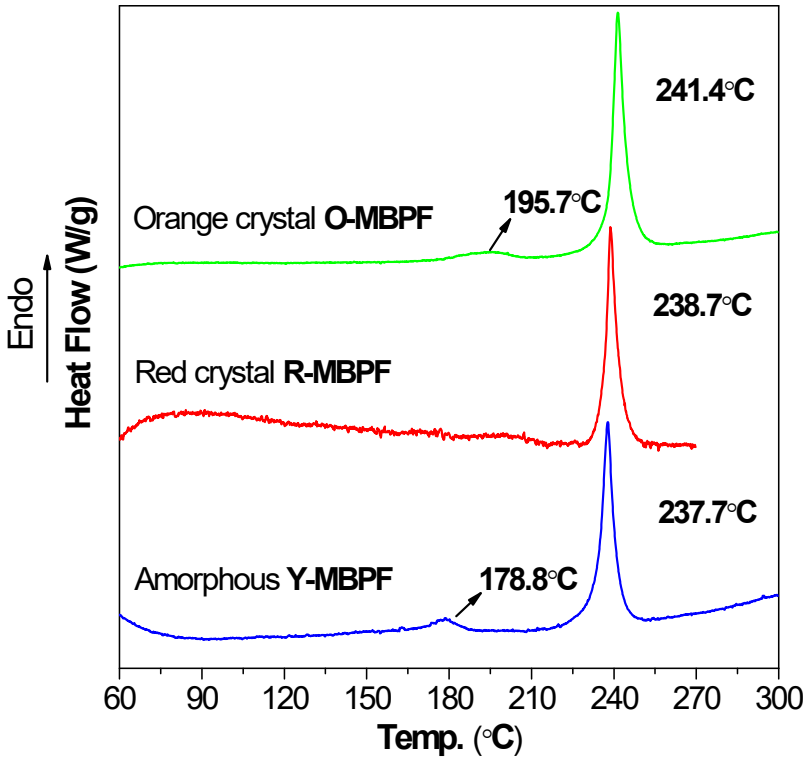

Fig. S12 DSC profiles of the orange crystal **O-MBPF**, red crystal **R-MBPF** and amorphous **Y-MBPF**.

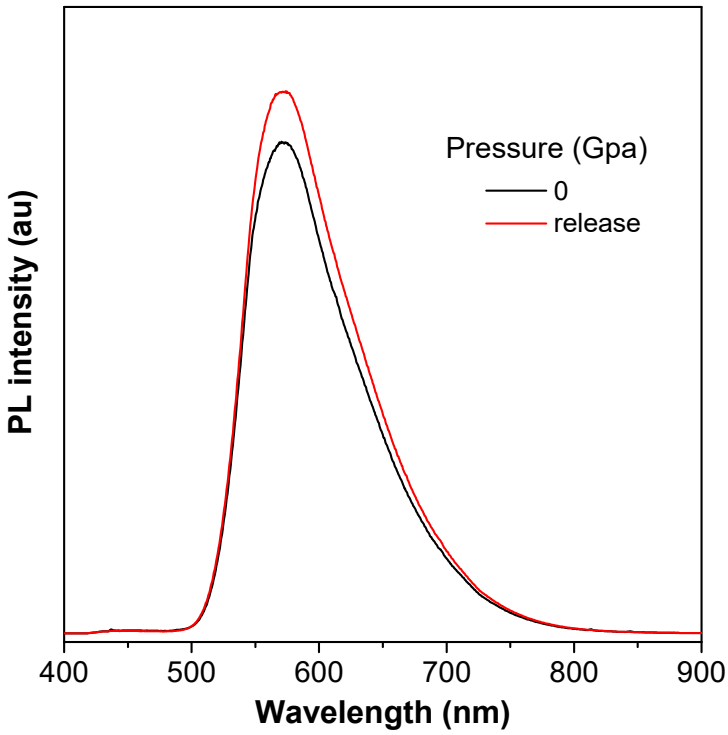

Fig. S13 The PL intensity of **MBPF** after release.

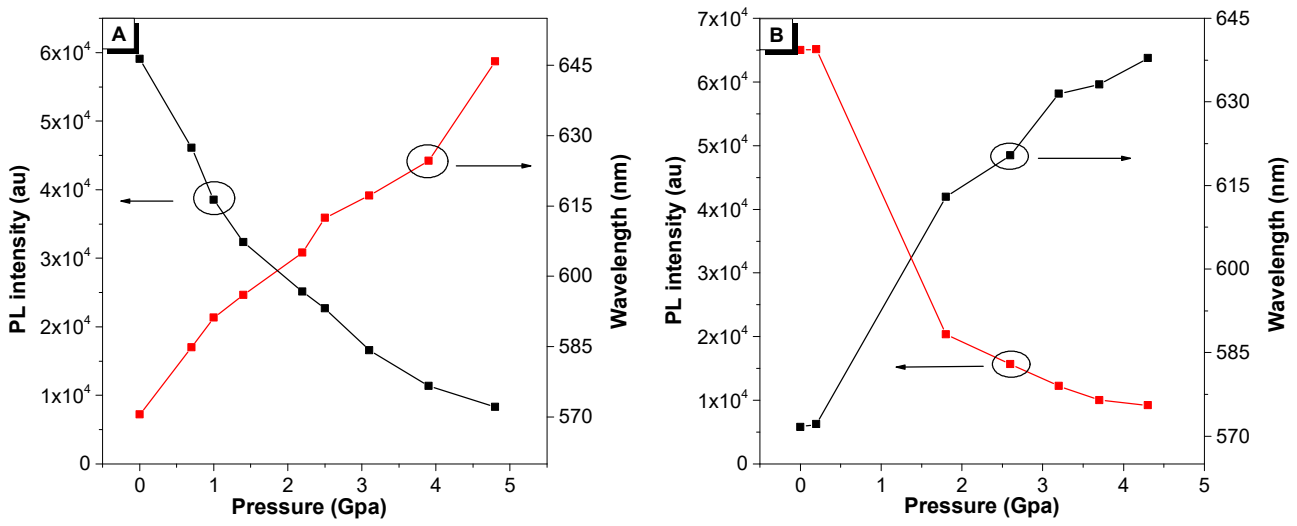

Fig, S14 Changes of PL intensity and wavelength of **R-MBPF** with increasing pressure (A) and decreasing pressure (B).

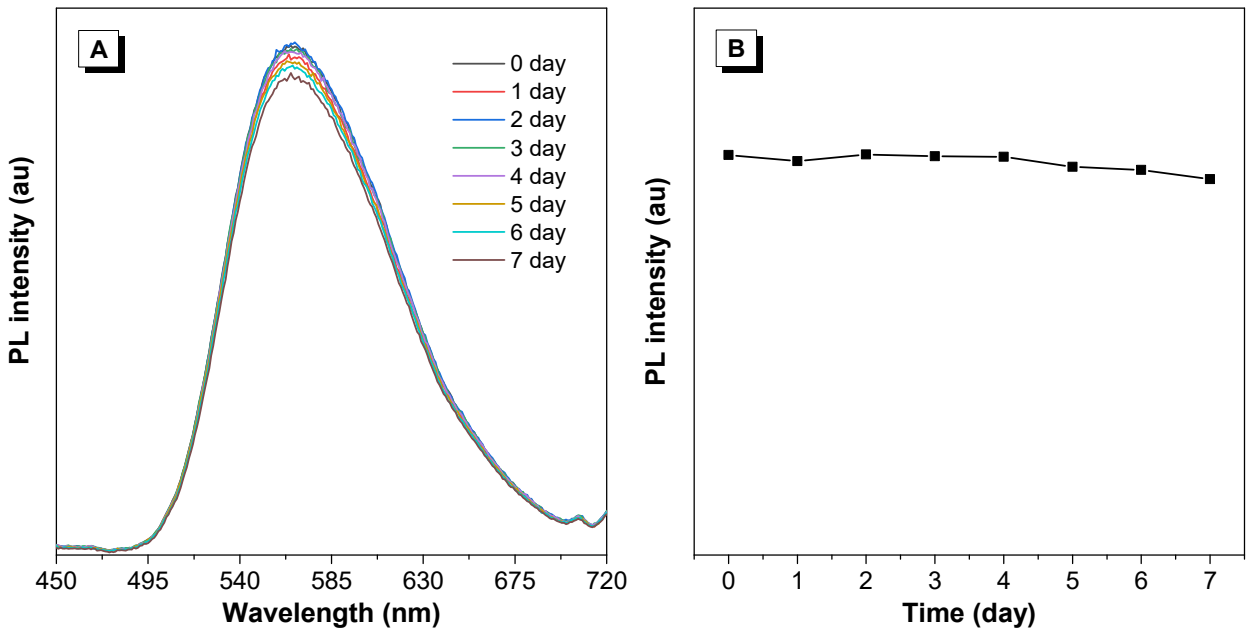

Fig. S15 Photostability of **MBPF** in 90% water/THF vs. storage time.

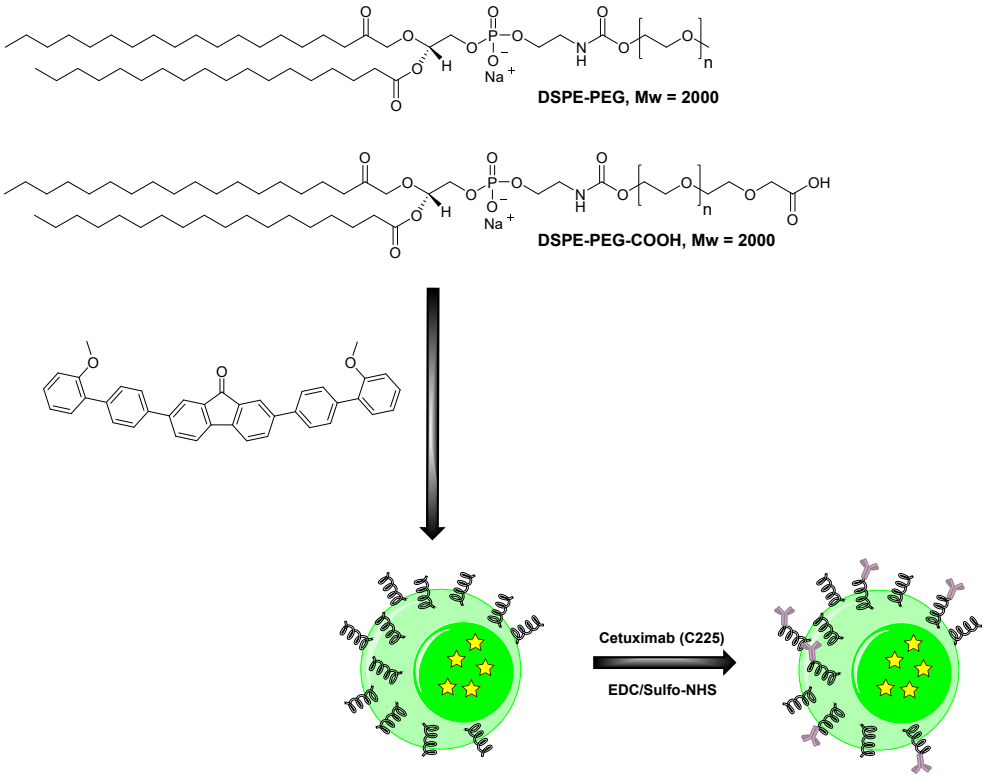

Scheme S2. Fabrication of **MBPF-C225** NPs.

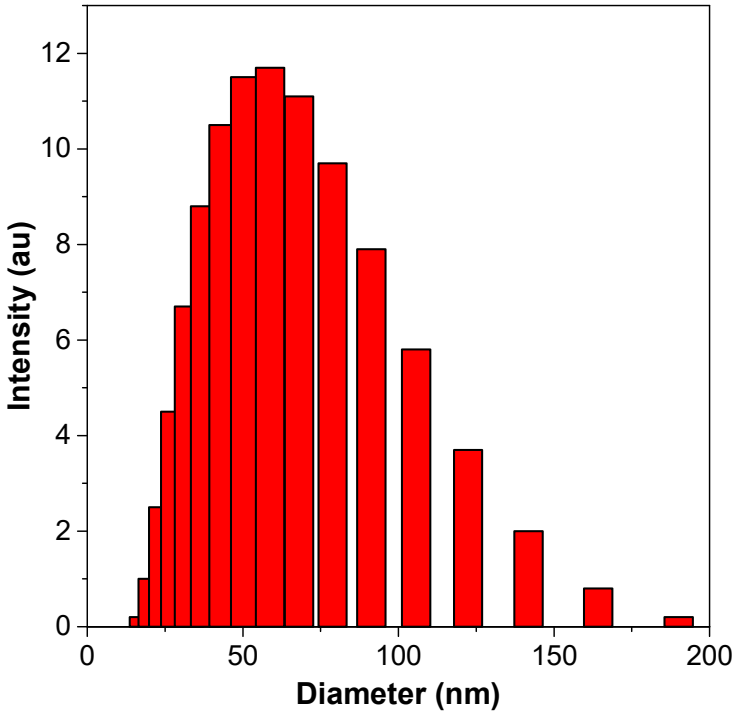

Fig. S16 Particle size distribution of **MBPF-C225** NPs studied by dynamic light scattering.

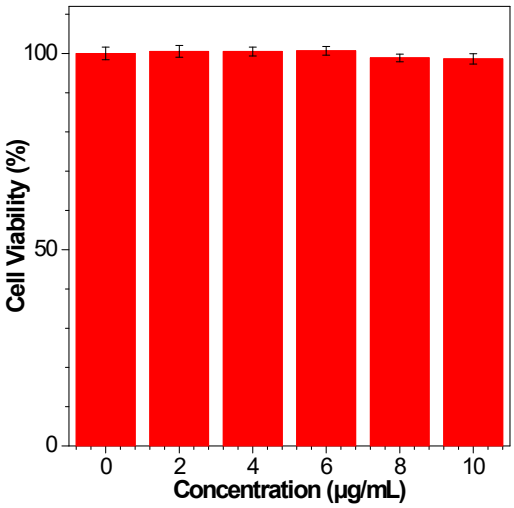

Fig. S17 Cell viability of HCC 827 cells treated with different concentrations of **MBPF-C225** NPs.

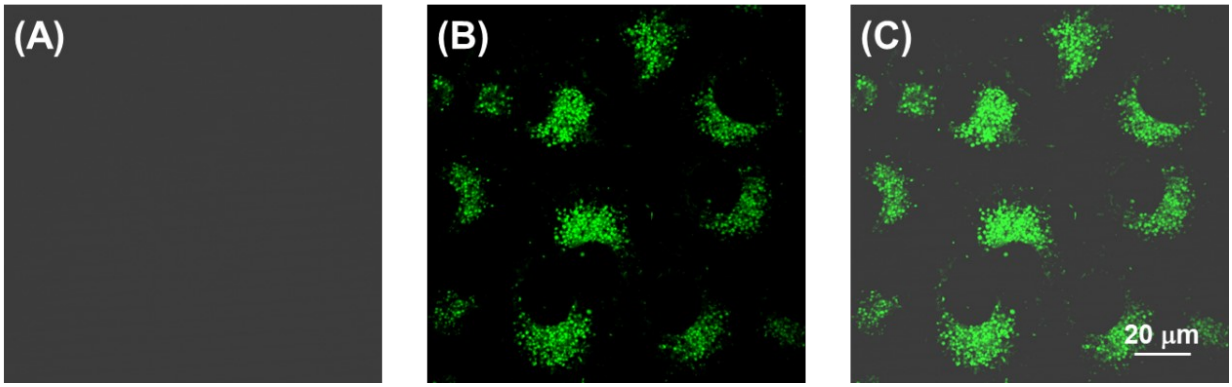

Fig. S18 The CLSM images of HCC827 cells after incubation with **MBPF-C225** NPs at 37 °C for 6 h. (A) Bright-field images; (B) fluorescence images; (C) the merged image of (A) and (B). Scale bar = 20 μm.

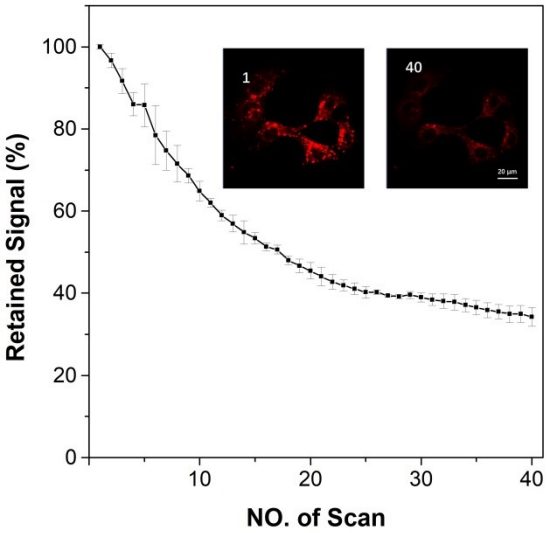

Fig. S19 Retained signal (%) of fluorescence of HCC827 cells stained with Lysotracker red with increasing number of scans. Inset: Fluorescence images of HCC827 cells with increasing number of scans (1 and 40 scans; the number of scans shown in upper left corner).